Published in final edited form as:
J Mol Biol. 2009 December 4; 394(3): 410–422. doi:10.1016/j.jmb.2009.08.067.

The Shuttling Protein Npl3 Promotes Translation Termination Accuracy in *Saccharomyces cerevisiae*

Luis A. Estrella[1], **Miles F. Wilkinson**[2], and **Carlos I. González**[1,*]

[1]Department of Biology, University of Puerto Rico, San Juan, Puerto Rico 00931

[2]Department of Biochemistry and Molecular Biology, The University of Texas M. D. Anderson Cancer Center, Houston, Texas 77030.

Abstract

Heterogeneous nuclear ribonucleoproteins (hnRNPs) are multi-functional proteins that bind to newly synthesized mRNAs in the nucleus and participate in many subsequent steps of gene expression. A well-studied *Saccharomyces cerevisiae* hnRNP that has several nuclear functions is Npl3p. Here, we provide evidence that Npl3p also has a cytoplasmic role: it functions in translation termination fidelity. Yeast harboring the *npl3-95* mutant allele have impaired ability to translate *LacZ*, enhanced sensitivity to cycloheximide and paromomycin, and increased ability to readthrough translation termination codons. Most of these defects are enhanced in yeast that also lack Upf1p, a factor crucial for the nonsense-mediated decay (NMD) RNA surveillance pathway that is also known to be involved in translation termination. We show that the *npl3-95* mutant allele encodes an Npl3p that forms high molecular-weight complexes that co-fractionate with the poly(A)-binding protein Pab1p. Together, the data suggest that Npl3p plays a role in translation termination in yeast.

INTRODUCTION

The original notion that gene expression is a series of independent steps has been replaced with the view that gene expression is a highly coupled pathway linked by key integrator molecules [1; 2]. For example, in the nucleus, the proteins required for mRNA capping are recruited to the transcription complex during transcription initiation, permitting mRNA capping to occur co-transcriptionally [3; 4]. Because the 5'-cap protects mRNAs from decay, it is crucial that capping occurs soon after the 5′-end of the mRNA is transcribed. Later events, such as mRNA splicing, cleavage, and polyadenylation, often also occur while a mRNA is still being transcribed [5; 6]. All these nuclear post-transcriptional events are coupled with transcription via the C-terminal domain (CTD) of the large subunit of RNA polymerase II (Pol II). The CTD achieves this by recruiting factors involved in all of these post-transcriptional events. Many other gene expression events in the nucleus are also coupled, including 5′-capping, splicing and polyadenylation [6; 7].

Following these nuclear processing events, transcripts must become competent for export across the nuclear pore [1; 4; 5; 8]. This competence is accomplished by the recruitment of specific RNA export factors and hnRNPs to newly synthesized transcripts. For example, the transcription export (TREX) complex, which binds the mRNA during transcriptional

*Corresponding author. Mailing address: Phone: (787) 764-0000 ext. 2482. Fax: (787) 764-4290. cigonzalez@uprrp.edu.

elongation, serves to promote RNA export [9; 10]. The Mex67p (TAP/NXF1 in vertebrates) protein is another important factor required for the export of mRNA to the cytoplasm [11]. Mex67p forms a heterodimeric export receptor with the protein Mtr2, which together interact with nuclear pore proteins and other adaptor RNA binding proteins to facilitate RNA movement across the nuclear pore [12; 13; 14].

Once in the cytoplasm, mRNAs undergo additional coupled events. For example, translation and cytoplasmic mRNA decay are linked, such that translation sometimes impedes decay and in other cases it accelerates decay. A quality control mechanism that may link both nuclear and cytoplasmic events is nonsense-mediated mRNA decay (NMD). This RNA surveillance mechanism recognizes and rapidly degrades mRNAs harboring premature (nonsense) termination codons (PTCs) [15; 16; 17]. NMD depends on several highly conserved factors, including Upf1, Upf2 and Upf3[18; 19; 20; 21; 22; 23]. The Upf proteins are involved not only in RNA surveillance but they also act in general translation and translation termination fidelity[19; 24; 25]. As evidence for the latter, deletion of any one of the three *UPF* genes leads to partial suppression of nonsense codon recognition [26; 27]. All together, during the process of gene expression a variety of factors associate with the mRNA to promote the translation of the encoded protein. Throughout this process, factors such as Mex67p associate during the mRNA export phase; whereas others, like the Upf proteins, bind to the mRNA upon export to the cytoplasm [16]. This constant exchange of factors that results in a highly dynamic mRNA molecule is commonly referred to messenger ribonucleoprotein (mRNP) remodeling [4].

In this paper, we focus on Npl3p, a well-studied multi-functional hnRNP that participates in many steps of gene expression. Npl3p interacts with the CTD of Pol II and directly stimulates the elongation activity of RNA polymerase II [28]. It also binds to pre-mRNA and promotes its processing by recruiting RNA splicing factors [29; 30; 31]. Following mRNA processing, Npl3p remains bound to the mRNA and actively promotes its export [32]. Recent evidence has suggested that Npl3p also functions in translation. Yeast cells harboring the *npl3-27* allele are defective in releasing the mutant form of Npl3p from translating polyribosomes and demonstrate impaired translation [33]. Furthermore, Npl3p copurifies with ribosomal proteins and the poly (A^+) mRNA binding protein, Pab1, both key components of the translational apparatus [33; 34]. Together, these results suggest that Npl3p is a good candidate to be a crucial factor that couples events in both the nucleus and the cytoplasm.

In this study, we address the role of Npl3p in translation. We provide evidence that a mutant form of Npl3p functions in translation termination fidelity. The translation termination defects observed in cells harboring a mutant allele of *NPL3* are enhanced by loss of a factor previously known to have a role in translation termination fidelity: Upf1p. Together, our results suggest that Npl3p plays a role in translation termination in yeast.

RESULTS

Evidence that Npl3p and Upf1p cooperate to facilitate translation in S. cerevisiae

Previous studies have demonstrated that Npl3p is recruited early during transcription and plays a role in many subsequent events, including transcription termination, 3′ end formation, mRNP assembly, and RNA export [29; 31; 35]. More recent studies have also linked Npl3p with translation, but a specific role for Npl3p in this process has not been elucidated [33]. To address this issue, we used *S. cerevisiae* strains harboring the *npl3-95*, *npl3-101* and *npl3-1* mutant alleles. The *npl3-95* mutant allele was originally identified as temperature-sensitive mutation that negatively silences the *HMR* locus [36]; it has also been shown to be required for mRNA export in yeast [32]. The *npl3-101* and *npl3-1* alleles were shown to mislocalize nuclear-bound proteins to other cellular compartments [32]. The mutations in these three alleles are all located within RNA recognition motif 2 (RRM2) of Npl3p (Fig. 1A). The *npl3* mutant alleles used in

this study share several phenotypes including: a) temperature sensitivity (Tsm^{-}) and b) defects in mRNA export. These phenotypes are only manifested at the restrictive temperature (≥28C °). Hence, the assays in this study were conducted at the permissive temperature (24C°) where no mRNA export defects are observed [32].

As a first test of whether Npl3p has a role in translation, we examined the sensitivity of these strains to the translation inhibitor cycloheximide. Previous studies have shown that yeast strains with translational defects are hypersensitive to the growth-inhibitory effects of this compound [37; 38]. As shown in Fig. 1B, the *npl3-95* strain was hypersensitive to cycloheximide, while the *npl3-101* and *npl3-1* strains were resistant to this translational inhibitor (Fig. 1B). The Npl3-95p was expressed at levels comparable to that of the wild type Npl3p (Fig. 1C), suggesting that the defect observed was a result of a functional deficiency in translation and not due to reduced protein levels.

To further investigate the role of Npl3p in translation, we tested whether Npl3p genetically interacts with Upf1p, a central component of the NMD RNA surveillance pathway that has a role in translation and is known to physically interact with the hnRNP family member Hrp1p [39]. In agreement with previous reports, we found that a strain harboring a deletion of the *UPF1* gene (*upf1Δ*) was sensitive to cycloheximide (Fig. 1B) [40]. The *upf1Δ* strain showed less sensitivity to this drug than the *npl3-95* strain. When the two mutations were combined, this elicited an enhanced growth defect in response to cycloheximide treatment relative to either the *upf1Δ* or *npl3-95* single-mutant strains (Fig. 1B). The synthetic enhancement of the cycloheximide sensitivity phenotype in the double-mutant (*npl3-95/upf1Δ*) strain supports the notion for a role of the Npl3-95p mutant in translation [41].

As an independent assay for detecting defects in protein synthesis, we transformed *npl3-95*, *npl3-101* and *npl3-1* strains with a β-galactosidase reporter and measured translation rates. The total activity for each strain was normalized to *lacZ* mRNA and expressed as β-galactosidase activity (data not shown). As shown in Fig. 2, the *npl3-95* strain exhibited a ~70% reduction in total *lacZ* activity compared to wild-type cells. This translation defect was allele specific, as cells harboring the *npl3-101* or *npl3-1* alleles did not exhibit reduced *lacZ* activity. The *upf1Δ* strain exhibited a less marked (~40%) reduction in total *lacZ* activity, while the double *npl3-95/upf1Δ* mutant strain exhibited a strong (~85%) reduction in total *lacZ* activity. These results suggest defects in translation of the *lacZ* mRNA in these strains and are consistent with the cycloheximide sensitivity phenotypes observed in Fig. 1B.

Npl3p and Upf1p are required for accurate translation termination

To determine whether Npl3p functions to promote translation by increasing its fidelity, we examined the effect of paromomycin on the growth phenotypes of the *npl3* mutant strains. This aminoglycoside increases the error rates of translating ribosomes; hence strains compromised for translational fidelity are hypersensitive to paromomycin [37; 42]. We found that the *npl3-95* strain was sensitive to paromomycin, indicative of a defect in translational fidelity in these cells (Fig. 3A). In contrast, the *npl3-101* and *npl3-1* strains did not show sensitivity to this translational inhibitor (Fig. 3A). In agreement with previous reports, we found that the growth of the *upf1Δ* strain was also sensitive to paromomycin; albeit less so (Fig. 3A). Analysis of the double-mutant (*npl3-95/upf1Δ*) strain revealed a synthetically enhanced sensitivity to paromomycin relative to the single-mutant strains. These results are consistent with the assay performed in the presence of cycloheximide (Fig. 1B) and the translational rates of *lacZ* reporters (Fig. 2), providing further evidence for a role of Npl3p in translation fidelity.

To determine whether Npl3p promotes translation fidelity during the elongating phase of translation, we used a dual-luciferase reporter construct previously developed to measure translation elongation fidelity [42]. This reporter construct contains *Renilla* and firefly luciferase

coding sequences in tandem, separated by a linker region (Fig. 3B). The firefly luciferase gene in this construct harbors a histidine-toarginine mutation (Arg245) within a catalytically important residue that, under normal conditions, generates an inactive form of firefly luciferase [42]. Cells with reduced translation elongation accuracy incorporate histidine at this position instead of arginine, resulting in the production of an active form of firefly luciferase. The misincorporation of histidine instead of arginine at this position occurs at relatively high frequency because the histidine-tRNA is the near-cognate tRNA for arginine. This system allows for an accurate measure of translation elongation fidelity by determining the activity of the firefly luciferase enzyme relative to the upstream *Renilla* luciferase activity [42]. Using this assay, we found that both *npl3-95* and wild-type strains expressed similar levels of firefly luciferase activity suggesting that *npl3-95* cells are not defective in translation elongation fidelity (Fig. 3C).

Given that Npl3p did not appear to function in translation elongation fidelity, we determined its role in translation termination. To test this, we used a dual-luciferase assay system previously developed to quantify translation termination efficiency [26]. This assay consists of a bicistronic reporter mRNA that contains the *Renilla* and the firefly luciferase in tandem, separated by a linker sequence that harbors a stop codon (Fig. 4). In yeast strains defective in translation termination, higher levels of firefly luciferase are synthesized due to a higher frequency of ribosomes readthrough of the stop codon. Therefore, an increase in activity of the firefly luciferase relative to the *Renilla* activity is directly proportional to defects in translation termination. Using this dual-luciferase assay, we quantitated the readthrough activity at all three stop codons. The *upf1Δ* strain expressed modestly higher levels of luciferase than the wild-type strain (by 3- and 2-fold for the UGA and UAG constructs, respectively; Fig. 4), in agreement with previous reports [26]. Under similar conditions, we were not able to observe translational readthrough activity for the *upf1Δ* strain harboring the UAA stop codon construct. Strikingly, *npl3-95* cells exhibited much more elevated readthrough activity (by 30-, 6-, and 4-fold for the UGA, UAG, and UAA constructs, respectively; Fig. 4) than *upf1Δ* cells, indicating that defects in Npl3p cause a much more profound defect in translation termination fidelity than loss of Upf1p. As was the case for cycloheximide, translational rates and paromomycin sensitivity (Figs. 1B, 2 & 3A, respectively), this effect was specific for the *npl3-95* allele, as the *npl3-1* and *npl3-101* strains did not have significantly higher luciferase activity than wild-type cells (Fig. 4). Double-mutant (*npl3-95/upf1Δ*) cells had higher luciferase activity than either single-mutant (*npl3-95 or upf1Δ*) strain (Fig. 4). The increased readthrough activity was greater than additive in the double-mutant cells as compared to the single-mutant cells at all three stop codons, implicating Npl3p in translation termination fidelity. Together with the data showing that the double-mutant strain had increased sensitivity to translation inhibitors (Fig. 1B & 3A), these results suggest that Npl3 is required to promote accurate translation termination.

Hmt1p and Sky1p do not play a role in translation termination

Npl3p, like other hnRNP proteins, is subjected to several post-translational modifications including methylation and phosphorylation [11; 43; 44]. The nuclear arginine methyl-transferase, Hmt1p, is involved in the methylation of the RGG domain of Npl3p. The methylation of these amino acid residues promotes nuclear-cytoplasmic shuttling of Npl3p [43; 45]. Deletion of Hmt1p is lethal in combination with several *npl3* mutant alleles, including *npl3-95*, a phenotype that may reflect an effect in a critical process such as translational accuracy [46]. Npl3p is also subjected to phosphorylation by the serine arginine (SR)-rich protein kinase Sky1p. This phosphorylation and dephosphorylation cycle allows Npl3p to disengage from the mRNA and shuttle back into the nuclear compartment [47; 48]. To determine whether Hmt1p or Sky1p are required for proper translation termination, we assessed the nonsense suppression phenotype of the *can1-100* allele (which contains an *UAA* premature termination codon) in these mutant

strains. In yeast strains defective in translation termination, nonsense codon readthrough produces a functional form of the arginine permease Can1p that is capable of importing canavanine, a toxic arginine analog. Therefore, decreased growth rates correlate with enhanced nonsense suppression activity. [49; 50]. As shown in Fig. 5, *hmt1Δ* or *sky1Δ* strains did not display nonsense suppression phenotypes. In contrast, the *npl3-95* and the *upf1Δ* mutant strains grew much more poorly (Can^s) in the presence of canavanine (Fig. 5), in agreement with the defects in translation termination observed in both strains (Figs. 3 & 4). The *upf1Δ* strain showed more sensitivity to canavanine than *npl3-95* due to the mRNA stabilizing effect on the *can1-100* transcript that occurs in *upf1Δ* strain (Fig. 5B). The stabilization of the *can1-100* NMD substrate provides for enhanced substrate availability and worse growth conditions for the *upf1Δ* strain. Therefore, these results are consistent with Npl3-95p mutant having a strong defect in translation termination. The results also indicate that Hmt1p or Sky1p do not appear to play a role in translation termination in yeast. Hence, the role of Npl3p in translation termination is independent of the post-translational modifications mediated by Hmt1p and/or Sky1p.

The translation-deficient mutant Npl3p forms high molecular-weight complexes associated with Pab1p

To determine whether the translational defects observed in cells harboring the *npl3-95* mutant are due to abnormalities in polyribosome formation, we compared the polysome profile of this mutant strain with the wild-type strain using sucrose density sedimentation. We found that the *npl3-95* strain exhibited a polysome profile very similar to that of wild-type cells (Fig. 6A). The finding that polysome formation was not significantly perturbed by the mutation in the *npl3-95* allele suggested that Npl3p does not function in steps that lead up to polysome formation (e.g., translation initiation) and was consistent with our data showing that this mutation did not affect translation elongation fidelity (Fig. 3C) but rather affected translation termination (Fig. 4).

Because a role in translation termination could affect Npl3p's association with polysomes, we next determined the distribution of Npl3p in sucrose gradients. We found that ~25% of wild-type Npl3p associated with the high-density fractions in sucrose gradients (lane 9 and above), consistent with a protein involved in translation (Fig. 6A). To determine whether the presence of Npl3p in such high-density fractions of the gradient was indicative of its association with polysomes, we monitored Npl3p distribution in the presence of EDTA. Previous studies have demonstrated that treatment of whole cell extracts with EDTA dissociates polysomes by disrupting the interaction between the 40S and 60S ribosomal subunits [19]. We found that treatment of lysates from wild-type cells with EDTA elicited a shift in Npl3p from the high-density fractions to lower fractions (lanes 1-8) such that only ~5% of it remained in the high-density fractions (Fig. 6B). Likewise, control proteins (Pab1p and the ribosomal protein Tcm1p) shifted towards the lighter fractions and were largely absent from the high-density fractions. Together, this data demonstrated that EDTA effectively disrupted the polysomes and that a significant fraction of Npl3p is normally associated with polysomes. This data also agreed with a previous study from Krebber and colleagues who found that ~30% of Npl3p associates with actively translating ribosomes [33].

The inability of the *Npl3-95* mutant to efficiently promote translation termination suggested that this mutant protein might have an altered association with polysomes. Consistent with this, we found that the *npl3-95* mutant strain expressed a form of Npl3p that was much more abundant in the high-density fractions than was wild-type Npl3p (Fig. 6A). More than 50% of the Npl3-95p mutant was found in the high-density fractions. To determine whether this was the result of an association with polysomes, we assayed whether EDTA would disrupt the association. Surprisingly, we found that the mutant Npl3p did not significantly shift from the high-density fractions when the lysates were treated with EDTA (Fig. 6B). Likewise, ~40%

of Pab1p remained in the high-density fraction of EDTA-treated lysates prepared from the mutant *npl3-95* strain (Fig. 6B). In marked contrast, only ~5% of Pab1p was in the high-density fraction of EDTA-treated lysates from cells harboring wild-type Npl3p. As a control, we examined the ribosomal protein Tcm1 and found that it shifted from the high-density fractions to the low-density fraction in response to EDTA treatment of both mutant and wild-type Npl3p lysates. Together, these results indicated that the Npl3-95p mutant co-sediments with high molecular-weight fractions that contain Pab1p but lack actively translating ribosomes.

To determine whether the Npl3p mutant and Pab1p co-fractionation depends on the presence of RNA, we treated the lysates with RNase A before sucrose gradient centrifugation. RNase treatment reduced the amount of Pab1p in the high-density fractions, whereas it had little or no effect on the amount of the Npl3p mutant in such fractions (Fig. 6C). This indicated that mutant Npl3p is probably an integral component of the high molecular-weight complexes, whereas Pab1p probably depends on interactions with the poly(A) tail of mRNA to be present in such complexes. In the Discussion, we speculate as to the nature of these high molecular-weight complexes.

DISCUSSION

In this study, we report that two proteins, Npl3p and Upf1p, previously shown to be involved at different steps of gene expression have a common function in translation termination. The mRNA-binding protein Npl3p functions in mRNA processing, transcription termination, and RNA export [28; 29; 31; 35], while the RNA helicase Upf1p is a central component of the NMD RNA surveillance pathway [51; 52; 53]. We provide several lines of evidence that Npl3p and Upf1p function in translation termination in yeast. First, cells harboring mutations either in Npl3p or Upf1p were hypersensitive to the translational inhibitors cycloheximide and paromomycin (Figs. 1B and 3A). Second, the general translation rates were reduced in both *npl3-95* and *upf1Δ* strains (Fig. 2). Third, a double *npl3-95/upf1Δ* mutant strain exhibited enhanced sensitivity to both of these translational inhibitors relative to the single-mutant (*npl3-95* or *upf1Δ*) strains. This effect was also observed in the general translation rates as measured by *lacZ* reporters (Fig. 2). Finally, a quantitative read-through assay using a dual-luciferase assay system[42] revealed an enhancement in translational readthrough activity (ranging from 12- to 60-fold) at all stop signals for the *npl3-95/upf1Δ* strain relative to the single-mutant strains (Fig. 4). Together, the results outlined above support the notion that Npl3p and Upf1p act to maintain accurate translation termination.

Notably, the translational defects observed in the *npl3-95* strain are allele specific in nature. The *npl3* alleles used in this study are located within the second RNA recognition motif (RRM2) of Npl3p (Fig. 1A). The *npl3-95* mutant allele encodes a leucine to tyrosine mutation at position 216 within RRM2 of Npl3p, found within the α-helix one of the RRM2 domain of Npl3p [32]. According to the available structural data, this helix packs against the back of the β-sheet which forms the RNA recognition surface [35]. However, it is not localized within the RNA binding surface itself, thus making the disruption of accurate protein-RNA interactions an unlikely scenario [35]. Interestingly, the residues that form the α-helix one are part of a heptapeptide repeat highly conserved among higher eukaryotic SR proteins such as SF2 and *Drosophila* SRp55 [32]. Mutational analysis of this region in SF2 have previously demonstrated a negative regulatory role of splicing *in vitro* 54. However, no significant inhibitory activity on splicing has been demonstrated for Npl3p. In contrast, the *npl3-101* mutant allele is found within the β-sheet that forms the RNA binding surface of the RRM2 changing a glycine residue at position 241 to aspartate [32]. This glycine at position 241 is predicted to be crucial for mRNA binding and a change to a negatively charged residue might be repulsive to the negatively charged mRNA molecule [55]. The *npl3-1* allele is located within α-helix 2 of the RRM2; this mutant represents a change in alanine 254 to a valine residue, conserving the hydrophobic

nature at this location [32]. Both mutations (*npl3-101* and *npl3-1*) do not show any defects in general translation or translation termination, underscoring the importance of the conserved heptapetide sequence found within the RRM2. The RRM motif is known to mediate multiple types of interactions including protein-RNA, RRM-RRM and protein-protein interactions[55; 56]. Therefore, the *npl3-95* mutant protein could be disrupting crucial protein-protein interactions that are necessary for accurate translational termination (e.g. aberrant Pab1p distribution observed in Fig. 6). This might explain the *npl3-95* allele specific translational defects observed in this study.

Previous reports have suggested that both Npl3p and Upf1p play a role in translation [19; 33]. In the case of Npl3p, it was previously shown to be physically associated with polysomes and proteins involved in translation, including Pab1p [9; 33]. Moreover, cells harboring a mutant form of Npl3p (*npl3-27*) are defective in releasing the mutant form of Npl3p from translating polyribosomes and demonstrate impaired mRNA translation [33]. Interestingly, the *npl3-27* allele resembles the *npl3-95* with regards to the defects observed in general translation and a robust presence in polyribosomal fractions. In contrast, the *npl3-27* mutation is located at the C-terminal region of the protein within the RGG domain (Fig. 1A) [33]. This region is crucial for the shuttling function of SR proteins, hence it is the region targeted for phosphorylation by the Sky1 protein kinase and methylation by the Hmt1 methylase [47]. However, our results do not suggest a role for these modifications in the process of translation termination (Fig. 5). Together, these results suggest that the RGG and RRM2 domains of Npl3p might play important roles in the process of translation. The data in our paper clarifies the role of Npl3p by providing strong evidence that it functions in translation termination fidelity (Figs.1, 2, 4). These results might indicate a potential defect for the *npl3-27* allele in nonsense suppression. However, dual luciferase assays fail to detect such effects (data not shown). This further underscores the allele specificity effects of *npl3-95* in translation termination.

We also confirmed that Upf1p has a role in translation termination (Figs. 1, 2, 4, 5) [19; 57]. Recent studies have suggested that human UPF1 also has role in translation: phosphorylated UPF1 interacts with eIF3, a translation initiation factor required for the recycling of post-termination complexes, and triggers repression during NMD [58]. It remains to be determined precisely how Npl3p and Upf1p function in translation termination fidelity. We found that the combination of mutations in both genes leads to a synthetic enhancement of the translational defects observed in either mutation alone (Figs. 1B, 2, 3A, 4, 5). The synthetic enhancement of the *npl3-95* translational defects by the deletion of *upf1Δ* further supports a role for Npl3p in translation termination.

We found that the translation-deficient mutant form of Npl3p (Npl3-95p) is associated with high molecular-weight fractions in sucrose density gradients raising the possibility that it may associate with high molecular-weight complexes (Fig. 6A). These complexes are unlikely to contain polysomes, as EDTA treatment had little effect on them (Fig. 6B). Strikingly, a significant fraction (40%) of Pab1p cosedimented with these high molecular-weight fractions in a RNA-dependent manner (Figs. 6B & 6C), suggesting that the *npl3-95* mutant strain harbors a form of Npl3p that might sequester Pab1p in large RNPs. Based on these observations, we propose that the Npl3-95p mutant protein promotes an aberrant mRNP conformation that can sequester Pab1p from the actively translating mRNA pool, thus compromising translation termination fidelity. Consistent with this idea, Pab1p has been previously implicated in the regulation of translation termination and is an important component of the translation machinery [59; 60]. Other proteins, including Npl3p-interacting proteins (e.g. Gbp2p, Hrb1p), might also be present in these high molecular-weight complexes and thereby contribute to the translation termination defect.

Our model also implies that a correct mRNP environment is a prerequisite for proper translation termination to occur [4; 61; 62]. Upf1p may have a role in creating this environment, as previous studies have suggested that Upf1p plays a role in mRNP remodeling [62]. We further hypothesize that the mRNP composition at the translation termination event requires the integrity of the machinery for proper termination to occur. The improper rearrangement of the mRNP due to shortage of Pab1p (titrated by the mutant Npl3-95p) at the termination event may provoke a delay in the change of the ribosome conformation(s) required for polypeptide chain release [63]. This, in turn, might open a window for a near cognate tRNA to enter the ribosomal-A site and promote translational readthrough [63].

Our studies suggest that Npl3p has a role in translation that is independent of its function in mRNA export [33], transcription and/or nuclear protein import [28; 29]. We hypothesize that other multi-functional proteins with similar roles to Npl3p might participate in this mRNP remodeling event. For example, recent studies have linked the RNA helicase, Dbp5 to mRNP remodeling and this factor is also required for translational fidelity [37; 64]. Therefore, factors such as TAP1/NXF1, Gle1 and Mex67 are potential candidates that might be involved in this nucleocytoplasmic coupling of mRNA export, translation and turnover [61; 64; 65]. In summary, our work establishes Npl3p as a multi-functional RNA-binding protein with functions that extend beyond the nucleus. Future studies will be required to determine precisely how Npl3p promotes translation termination fidelity in the cytoplasm.

METHODS

Yeast strains, growth media and plasmids

All strains used in this study are derived from the W303 genetic background. The genotypes of all yeast strains used in this study are listed in Table 1. Yeast strains were routinely grown at 24°C on either standard yeast extract/peptone (YP) medium or synthetic medium supplemented with appropriate amino acids and 2% dextrose as carbon source [66]. Genetic manipulations were performed via PCR-mediated gene disruption and correct integration confirmed by PCR [67]. The presence of the *can1-100* allele was confirmed by PCR amplification of the *CAN1* locus and DNA sequencing. Canavanine (250 μg/ml), cycloheximide (0.05 μg/ml, 0.075 μg/ml and 0.1 μg/ml) and paromomycin (0.25 mg/ml to 1 mg/ml) were added to the autoclaved YPD medium. Yeast transformations were performed by the lithium acetate procedure and plasmids were maintained by growth in selective media [66; 68]. Plasmids used in this study are listed in Table 2.

RNA isolation and Northern blotting

Total RNA was isolated via the hot acid phenol method and mRNA abundance was determined by Northern blot analysis as described previously [39; 69]. Briefly, 50 ml of yeast cells were grown at 24°C to OD_{600} of 0.6-0.8. Cells were centrifuged, washed twice in RNA extraction buffer (0.3M Sodium acetate, 50mM Tris pH 8.0, 5mM EDTA, 1% SDS) and resuspended in 400μl of RNA extraction buffer and equal volume of hot saturated phenol (phenol pH 6.8). The mixtures were incubated at 65°C for 5 minutes with vortex every minute, followed by centrifugation (15,682 *g*) at 4°C. This procedure was repeated twice and following centrifugation, the aqueous phase was extracted with RNA phenol (phenol-chloroform-isoamyl alcohol 125:24:1, pH 4.3). The supernatant was collected and one ml of ice cold 100% ethanol was added to the supernatant to precipitate the RNA. RNA samples were then centrifuged for 30 minutes at 15,682 *g* at 4°C. Pellets were washed with 70% ethanol and vacuum dried before resuspension in 50 μl of 10 mM Tris pH 7.5. Random-primed probes were prepared from PCR-amplified fragments of *CAN1*, *LacZ*, and *U3* to high specific activity with ^{32}P-dCTP following the recommendations from the manufacturer (Roche). The results from these studies were quantified using a Molecular Imager FX (BioRad, Hercules, CA). The values shown represent

the average of at least three independent experiments. Statistical analysis was performed using GraphPad Prism 5 software.

β-galactosidase assays

Yeast cultures (50 ml) were grown to OD_{600} of 0.6-0.8 at 24°C. One-half of the culture was used for total RNA isolation as described above. The second half of the culture was used for protein isolation. Cells were lysed with glass beads (0.5 μm in diameter) in breaking buffer (100 mM Tris-HCl [pH 8], 1 mM dithiothreitol, 20% glycerol; 2 mM phenylmethylsulfonyl fluoride and 1X protease inhibitor cocktail). Extracts were cleared by centrifugation (15,682 *g*) for ten minutes and protein concentrations were determined using the Bradford method. β-galactosidase liquid assays were performed by assaying each extract twice on Z buffer (using 200 μl of 4 mg/ml ONPG substrate. After thirty minutes, the reactions were stopped by adding 500 μl 1M Na_2CO_3. β-galactosidase activities shown represent at least three independent transformants per yeast strain and are expressed according to the following formula: (1.7 ml × OD_{420} units)/(0.0045 × cell extract volume [milliliters] × reaction time [minutes] × protein concentration [milligrams per milliliter]) [66; 70]. Statistical analysis was performed using GraphPad Prism 5 software.

Dual luciferase assays

Dual luciferase assays were performed with the dual luciferase reporter assay system (Promega Corp., Madison, WI) as described previously with minor modifications [42; 71]. Cells were grown to mid-logarithmic phase (OD_{600} 0.8) in SC-Ura medium. Ten microliters of cells were removed directly from the culture and transferred to 100 μl of 1x passive lysis buffer. After allowing lysis for 15 seconds, 10 μls were used for luminescence measurements using a TD-20/20 luminometer (Tuner Designs, Sunnyville, CA.). The following steps were used for luminescence measurements: 10 μl of the firefly luciferase reagent (LARII) were added to the sample with a 2 seconds equilibration time and measurement of luminescence with a 10 seconds integration time, followed by addition of 10 μl of the *Renilla* luciferase reagent and firefly quenching (Stop & Glo), 2 seconds equilibration time, and measurement of luminescence with a 10 seconds integration time. The values shown represent the ratio of the firefly luciferase activity to the *Renilla* activity of the stop codon-containing constructs divided by the ratio of the firefly luciferase activity to the *Renilla* activity of the sense codon-containing construct multiplied by 100. For misincorporation assays, cells were treated and processed in a similar manner. For each strain at least three independent transformants were assayed and each individual extract was scored for luminescence activity in triplicates. Statistical analysis was performed using GraphPad Prism 5 software.

Whole cell extract preparation

Yeast cell cultures (50ml) were grown at 24°C to mid-logarithmic phase and harvested by centrifugation. Cell pellets were washed twice in lysis buffer (50 mM Tris-HCl [pH 7.5], 100 mM NaCl, 5 mM EDTA, 10% glycerol, 1% Triton X-100) containing 1 mM PMSF and 1X protease inhibitor cocktail (Sigma) and transferred to microcentrifuge tubes. Cells were then resuspended in 250 μl of lysis buffer and 1/3 volume of 0.5 μm glass beads were added for mechanical lysis. Cells were vortexed six times for 30s at maximum speed with 2 minutes intervals on ice. Cell lysates were collected and cleared by centrifugation at 15,682 *g* for 10 minutes at 4°C. The cleared lysates were quantified using standard Bradford protein assay (Bio-Rad).

Western blot analysis

Yeast whole cell extracts were resolved by sodium dodecyl sulfate-polyacrylamide gel electrophoresis (SDS-PAGE). Briefly, protein samples were mixed with appropriate amounts

of 6X SDS-loading buffer and boiled for 5 minutes before loading onto a 10% SDS-PAGE gel and electrophoresed at 100V for 1.5 hours. The gel was then transferred to a nitrocellulose membrane (Bio-Rad) and blocked in 10% non-fat milk for 1 hour. The antibodies utilized were α-Npl3 (1:3000)[45], α-Tcm1 (1:2500) [72] (kindly provided by Dr. Michael F. Henry and Dr. Allan Jacobson) and α-Pab1 (1:5000). Their corresponding secondary antibodies were used in 1:10,000 dilutions. Membranes were developed using the Western Dura chemiluminescense kit (Pierce).

Sucrose density gradient fractionations

Sucrose density gradients were performed essentially as previously described [18]. Yeast cells (100 ml) were grown at 24°C in YPD medium to OD_{600} of 0.6. Cycloheximide was added to 100 μg/ml and incubated on ice for 10 minutes with occasional shaking [18]. Cells were harvested at 835 *g* for five minutes and washed with 50 ml of polysomes lysis buffer (10 mM Tris-Cl pH 7.5, 100 mM NaCl, 30 mM $MgCl_2$). After a second centrifugation, cells were resuspended in 10 mL of polysomes lysis buffer, centrifuged and the cell pellet was resuspended in one ml of lysis buffer. Glass beads (2/3 of the cell volume) were added to the samples and cells were lysed by vortexing 8 times for 15 seconds with a 30 seconds cool down period on ice. Lysates were centrifuged at 5,938 *g* for 5 minutes at 4°C; supernatants were collected and centrifuged at 11,228 *g* for 5 minutes at 4°C. Twenty OD_{260} units were loaded on 9ml 10-50% sucrose gradients. These gradients were centrifuged at 209,678 *g* for 3 hours at 4°C in an Optima L-100 XP ultracentrifuge (Beckman) using a SW 41 Ti rotor. Two- hundred microliter fractions were collected from the top of the sucrose gradients and their OD_{260nm} monitored via spectrophotometry. Fractions were pooled and precipitated with acetone and resuspended in 1X-SDS protein sample buffer. Samples were incubated for 10 min at 22°. For the experiments in the presence of EDTA, the lysis buffer and the sucrose gradient contained EDTA to a final concentration of 15 mM. For the RNaseA studies, the extract was pre-incubated with RNaseA to a final concentration of 0.1 mg/ml at 24°C for 20 minutes before loading to the sucrose gradient. The fractions were resolved in a 10-20% Criterion™ precast gel (Bio-Rad), transferred to nitrocellulose membranes and analyzed by Western Blotting as described above. The percentage of ribosomal association was calculated by quantifying the total amount of protein distributed in Western blot lanes 9 thru 15 divided by the total amount of the protein in the fifteen lanes multiplied by 100.

Acknowledgments

We are very grateful to Dr. David Bedwell for the gift of plasmids and strains, Dr. Allan Jacobson for the anti-Tcm1 antibody, Dr. Michael F. Henry for Npl3 plasmids, anti-Npl3 antibody, yeast strains and helpful discussions. We also thank members of the González laboratory for helpful comments. We also thank the Biostatistics Core of the U54 grant for their assistance. This work was supported by grants from the National Institutes of Health to C.I.G. (GM008102-3052, KO1 HL-04355-05, U54 CA96297, FIPI), M.F.W. (GM058595, U54 CA96297). This publication was made possible by Grant P20 RR 016174 from the National Center for Research Resources (NCRR), a component of the National Institutes of Health (NIH). Its contents are solely the responsibility of the authors and do not necessarily represent the official view of NCRR or NIH.

GLOSSARY

mRNP, messenger ribonucleoprotein; NMD, nonsense mediated mRNA decay; RRM, RNA recognition motif.

REFERENCES

1. Stewart M. Ratcheting mRNA out of the nucleus. Mol Cell 2007;25:327–30. [PubMed: 17289581]
2. Cole CN, Scarcelli JJ. Transport of messenger RNA from the nucleus to the cytoplasm. Curr Opin Cell Biol 2006;18:299–306. [PubMed: 16682182]

3. Ares M Jr, Proudfoot NJ. The spanish connection: transcription and mRNA processing get even closer. Cell 2005;120:163–6. [PubMed: 15680322]
4. Aguilera A. Cotranscriptional mRNP assembly: from the DNA to the nuclear pore. Curr Opin Cell Biol 2005;17:242–50. [PubMed: 15901492]
5. Moore MJ, Proudfoot NJ. Pre-mRNA processing reaches back to transcription and ahead to translation. Cell 2009;136:688–700. [PubMed: 19239889]
6. Goldstrohm AC, Greenleaf AL, Garcia-Blanco MA. Co-transcriptional splicing of pre-messenger RNAs: considerations for the mechanism of alternative splicing. Gene 2001;277:31–47. [PubMed: 11602343]
7. Le Hir H, Izaurralde E, Maquat LE, Moore MJ. The spliceosome deposits multiple proteins 20-24 nucleotides upstream of mRNA exon-exon junctions. Embo J 2000;19:6860–9. [PubMed: 11118221]
8. Cole CN, Scarcelli JJ. Unravelling mRNA export. Nat Cell Biol 2006;8:645–7. [PubMed: 16820771]
9. Hurt E, Luo MJ, Rother S, Reed R, Strasser K. Cotranscriptional recruitment of the serine-arginine-rich (SR)-like proteins Gbp2 and Hrb1 to nascent mRNA via the TREX complex. Proc Natl Acad Sci U S A 2004;101:1858–62. [PubMed: 14769921]
10. Katahira J, Yoneda Y. Roles of the TREX complex in nuclear export of mRNA. RNA Biol 2009;6
11. Gilbert W, Guthrie C. The Glc7p nuclear phosphatase promotes mRNA export by facilitating association of Mex67p with mRNA. Mol Cell 2004;13:201–12. [PubMed: 14759366]
12. Yao W, Lutzmann M, Hurt E. A versatile interaction platform on the Mex67-Mtr2 receptor creates an overlap between mRNA and ribosome export. EMBO J 2008;27:6–16. [PubMed: 18046452]
13. Yao W, Roser D, Kohler A, Bradatsch B, Bassler J, Hurt E. Nuclear export of ribosomal 60S subunits by the general mRNA export receptor Mex67-Mtr2. Mol Cell 2007;26:51–62. [PubMed: 17434126]
14. Senay C, Ferrari P, Rocher C, Rieger KJ, Winter J, Platel D, Bourne Y. The Mtr2-Mex67 NTF2-like domain complex. Structural insights into a dual role of Mtr2 for yeast nuclear export. J Biol Chem 2003;278:48395–403. [PubMed: 14504280]
15. Gonzalez CI, Bhattacharya A, Wang W, Peltz SW. Nonsense-mediated mRNA decay in Saccharomyces cerevisiae. Gene 2001;274:15–25. [PubMed: 11674994]
16. Maquat LE. Nonsense-mediated mRNA decay: splicing, translation and mRNP dynamics. Nat Rev Mol Cell Biol 2004;5:89–99. [PubMed: 15040442]
17. Maquat LE. Nonsense-mediated mRNA decay in mammals. J Cell Sci 2005;118:1773–6. [PubMed: 15860725]
18. Atkin AL, Schenkman LR, Eastham M, Dahlseid JN, Lelivelt MJ, Culbertson MR. Relationship between yeast polyribosomes and Upf proteins required for nonsense mRNA decay. J Biol Chem 1997;272:22163–72. [PubMed: 9268361]
19. Atkin AL, Altamura N, Leeds P, Culbertson MR. The majority of yeast UPF1 co-localizes with polyribosomes in the cytoplasm. Mol Biol Cell 1995;6:611–25. [PubMed: 7545033]
20. Shirley RL, Ford AS, Richards MR, Albertini M, Culbertson MR. Nuclear import of Upf3p is mediated by importin-alpha/-beta and export to the cytoplasm is required for a functional nonsense-mediated mRNA decay pathway in yeast. Genetics 2002;161:1465–82. [PubMed: 12196393]
21. Maderazo AB, Belk JP, He F, Jacobson A. Nonsense-containing mRNAs that accumulate in the absence of a functional nonsense-mediated mRNA decay pathway are destabilized rapidly upon its restitution. Mol Cell Biol 2003;23:842–51. [PubMed: 12529390]
22. He F, Jacobson A. Upf1p, Nmd2p, and Upf3p regulate the decapping and exonucleolytic degradation of both nonsense-containing mRNAs and wild-type mRNAs. Mol Cell Biol 2001;21:1515–30. [PubMed: 11238889]
23. Bhalla AD, Gudikote JP, Wang J, Chan WK, Chang YF, Olivas OR, Wilkinson MF. Nonsense codons trigger an RNA partitioning shift. J Biol Chem 2009;284:4062–72. [PubMed: 19091751]
24. Wang W, Czaplinski K, Rao Y, Peltz SW. The role of Upf proteins in modulating the translation read-through of nonsense-containing transcripts. Embo J 2001;20:880–90. [PubMed: 11179232]
25. Nott A, Le Hir H, Moore MJ. Splicing enhances translation in mammalian cells: an additional function of the exon junction complex. Genes Dev 2004;18:210–22. [PubMed: 14752011]

26. Keeling KM, Lanier J, Du M, Salas-Marco J, Gao L, Kaenjak-Angeletti A, Bedwell DM. Leaky termination at premature stop codons antagonizes nonsense-mediated mRNA decay in S. cerevisiae. Rna 2004;10:691–703. [PubMed: 15037778]
27. Weng Y, Czaplinski K, Peltz SW. Identification and characterization of mutations in the UPF1 gene that affect nonsense suppression and the formation of the Upf protein complex but not mRNA turnover. Mol Cell Biol 1996;16:5491–506. [PubMed: 8816462]
28. Dermody JL, Dreyfuss JM, Villen J, Ogundipe B, Gygi SP, Park PJ, Ponticelli AS, Moore CL, Buratowski S, Bucheli ME. Unphosphorylated SR-like protein Npl3 stimulates RNA polymerase II elongation. PLoS ONE 2008;3:e3273. [PubMed: 18818768]
29. Bucheli ME, Buratowski S. Npl3 is an antagonist of mRNA 3' end formation by RNA polymerase II. EMBO J 2005;24:2150–60. [PubMed: 15902270]
30. Bucheli ME, He X, Kaplan CD, Moore CL, Buratowski S. Polyadenylation site choice in yeast is affected by competition between Npl3 and polyadenylation factor CFI. RNA 2007;13:1756–64. [PubMed: 17684230]
31. Kress TL, Krogan NJ, Guthrie C. A single SR-like protein, Npl3, promotes pre-mRNA splicing in budding yeast. Mol Cell 2008;32:727–34. [PubMed: 19061647]
32. Henry M, Borland CZ, Bossie M, Silver PA. Potential RNA binding proteins in Saccharomyces cerevisiae identified as suppressors of temperature-sensitive mutations in NPL3. Genetics 1996;142:103–15. [PubMed: 8770588]
33. Windgassen M, Sturm D, Cajigas IJ, Gonzalez CI, Seedorf M, Bastians H, Krebber H. Yeast shuttling SR proteins Npl3p, Gbp2p, and Hrb1p are part of the translating mRNPs, and Npl3p can function as a translational repressor. Mol Cell Biol 2004;24:10479–91. [PubMed: 15542855]
34. Sachs AB, Varani G. Eukaryotic translation initiation: there are (at least) two sides to every story. Nat Struct Biol 2000;7:356–61. [PubMed: 10802729]
35. Deka P, Bucheli ME, Moore C, Buratowski S, Varani G. Structure of the yeast SR protein Npl3 and Interaction with mRNA 3'-end processing signals. J Mol Biol 2008;375:136–50. [PubMed: 18022637]
36. Loo S, Laurenson P, Foss M, Dillin A, Rine J. Roles of ABF1, NPL3, and YCL54 in silencing in Saccharomyces cerevisiae. Genetics 1995;141:889–902. [PubMed: 8582634]
37. Gross T, Siepmann A, Sturm D, Windgassen M, Scarcelli JJ, Seedorf M, Cole CN, Krebber H. The DEAD-box RNA helicase Dbp5 functions in translation termination. Science 2007;315:646–9. [PubMed: 17272721]
38. Salas-Marco J, Bedwell DM. GTP hydrolysis by eRF3 facilitates stop codon decoding during eukaryotic translation termination. Mol Cell Biol 2004;24:7769–78. [PubMed: 15314182]
39. Gonzalez CI, Ruiz-Echevarria MJ, Vasudevan S, Henry MF, Peltz SW. The yeast hnRNP-like protein Hrp1/Nab4 marks a transcript for nonsense-mediated mRNA decay. Mol Cell 2000;5:489–99. [PubMed: 10882134]
40. Leeds P, Wood JM, Lee BS, Culbertson MR. Gene products that promote mRNA turnover in Saccharomyces cerevisiae. Mol Cell Biol 1992;12:2165–77. [PubMed: 1569946]
41. Guarente L. Synthetic enhancement in gene interaction: a genetic tool come of age. Trends Genet 1993;9:362–6. [PubMed: 8273152]
42. Salas-Marco J, Bedwell DM. Discrimination between defects in elongation fidelity and termination efficiency provides mechanistic insights into translational readthrough. J Mol Biol 2005;348:801–15. [PubMed: 15843014]
43. McBride AE, Cook JT, Stemmler EA, Rutledge KL, McGrath KA, Rubens JA. Arginine methylation of yeast mRNA-binding protein Npl3 directly affects its function, nuclear export, and intranuclear protein interactions. J Biol Chem 2005;280:30888–98. [PubMed: 15998636]
44. Shen EC, Henry MF, Weiss VH, Valentini SR, Silver PA, Lee MS. Arginine methylation facilitates the nuclear export of hnRNP proteins. Genes Dev 1998;12:679–91. [PubMed: 9499403]
45. Xu C, Henry MF. Nuclear export of hnRNP Hrp1p and nuclear export of hnRNP Npl3p are linked and influenced by the methylation state of Npl3p. Mol Cell Biol 2004;24:10742–56. [PubMed: 15572678]
46. Shen EC, Stage-Zimmermann T, Chui P, Silver PA. 7The yeast mRNA-binding protein Npl3p interacts with the cap-binding complex. J Biol Chem 2000;275:23718–24. [PubMed: 10823828]

47. Gilbert W, Siebel CW, Guthrie C. Phosphorylation by Sky1p promotes Npl3p shuttling and mRNA dissociation. Rna 2001;7:302–13. [PubMed: 11233987]
48. Yun CY, Fu XD. Conserved SR protein kinase functions in nuclear import and its action is counteracted by arginine methylation in Saccharomyces cerevisiae. J Cell Biol 2000;150:707–18. [PubMed: 10952997]
49. Maderazo AB, He F, Mangus DA, Jacobson A. Upf1p control of nonsense mRNA translation is regulated by Nmd2p and Upf3p. Mol Cell Biol 2000;20:4591–603. [PubMed: 10848586]
50. Ono BI, Ishino Y, Shinoda S. Nonsense mutations in the can1 locus of Saccharomyces cerevisiae. J Bacteriol 1983;154:1476–9. [PubMed: 6343355]
51. Cui Y, Hagan KW, Zhang S, Peltz SW. Identification and characterization of genes that are required for the accelerated degradation of mRNAs containing a premature translational termination codon. Genes Dev 1995;9:423–36. [PubMed: 7883167]
52. Ruiz-Echevarria MJ, Czaplinski K, Peltz SW. Making sense of nonsense in yeast. Trends Biochem Sci 1996;21:433–8. [PubMed: 8987399]
53. He F, Brown AH, Jacobson A. Upf1p, Nmd2p, and Upf3p are interacting components of the yeast nonsense-mediated mRNA decay pathway. Mol Cell Biol 1997;17:1580–94. [PubMed: 9032286]
54. Birney E, Kumar S, Krainer AR. Analysis of the RNA-recognition motif and RS and RGG domains: conservation in metazoan pre-mRNA splicing factors. Nucleic Acids Res 1993;21:5803–16. [PubMed: 8290338]
55. Maris C, Dominguez C, Allain FH. The RNA recognition motif, a plastic RNA-binding platform to regulate post-transcriptional gene expression. Febs J 2005;272:2118–31. [PubMed: 15853797]
56. Kielkopf CL, Lucke S, Green MR. U2AF homology motifs: protein recognition in the RRM world. Genes Dev 2004;18:1513–26. [PubMed: 15231733]
57. Czaplinski K, Weng Y, Hagan KW, Peltz SW. Purification and characterization of the Upf1 protein: a factor involved in translation and mRNA degradation. Rna 1995;1:610–23. [PubMed: 7489520]
58. Isken O, Kim YK, Hosoda N, Mayeur GL, Hershey JW, Maquat LE. Upf1 phosphorylation triggers translational repression during nonsense-mediated mRNA decay. Cell 2008;133:314–27. [PubMed: 18423202]
59. Cosson B, Couturier A, Chabelskaya S, Kiktev D, Inge-Vechtomov S, Philippe M, Zhouravleva G. Poly(A)-binding protein acts in translation termination via eukaryotic release factor 3 interaction and does not influence [PSI(+)] propagation. Mol Cell Biol 2002;22:3301–15. [PubMed: 11971964]
60. Brune C, Munchel SE, Fischer N, Podtelejnikov AV, Weis K. Yeast poly(A)-binding protein Pab1 shuttles between the nucleus and the cytoplasm and functions in mRNA export. Rna 2005;11:517–31. [PubMed: 15769879]
61. Kutay U, Panse VG. Gle1 does double duty. Cell 2008;134:564–6. [PubMed: 18724928]
62. Hilleren P, Parker R. mRNA surveillance in eukaryotes: kinetic proofreading of proper translation termination as assessed by mRNP domain organization? Rna 1999;5:711–9. [PubMed: 10376871]
63. Pape T, Wintermeyer W, Rodnina MV. Conformational switch in the decoding region of 16S rRNA during aminoacyl-tRNA selection on the ribosome. Nat Struct Biol 2000;7:104–7. [PubMed: 10655610]
64. Weirich CS, Erzberger JP, Flick JS, Berger JM, Thorner J, Weis K. Activation of the DExD/H-box protein Dbp5 by the nuclear-pore protein Gle1 and its coactivator InsP6 is required for mRNA export. Nat Cell Biol 2006;8:668–76. [PubMed: 16783364]
65. Alcazar-Roman AR, Tran EJ, Guo S, Wente SR. Inositol hexakisphosphate and Gle1 activate the DEAD-box protein Dbp5 for nuclear mRNA export. Nat Cell Biol 2006;8:711–6. [PubMed: 16783363]
66. Sherman F. Getting started with yeast. Methods Enzymol 2002;350:3–41. [PubMed: 12073320]
67. Longtine MS, McKenzie A, Demarini DJ, Shah NG, Wach A, Brachat A, Philippsen P, Pringle JR. Additional modules for versatile and economical PCR-based gene deletion and modification in Saccharomyces cerevisiae. Yeast (3rd) 1998;14:953–61. [PubMed: 9717241]
68. Gietz RD, Schiestl RH. High-efficiency yeast transformation using the LiAc/SS carrier DNA/PEG method. Nat Protoc 2007;2:31–4. [PubMed: 17401334]

69. Wang W, Cajigas IJ, Peltz SW, Wilkenson MF, Gonzalez CI. Role of Upf2 phosphorylation in Saccharomyces cerevisiae Nonsence-Mediated Decay. MCB. 2006

70. Pappas DL Jr, Hampsey M. Functional interaction between Ssu72 and the Rpb2 subunit of RNA polymerase II in Saccharomyces cerevisiae. Mol Cell Biol 2000;20:8343–51. [PubMed: 11046131]

71. McNabb DS, Reed R, Marciniak RA. Dual luciferase assay system for rapid assessment of gene expression in Saccharomyces cerevisiae. Eukaryot Cell 2005;4:1539–49. [PubMed: 16151247]

72. Mangus DA, Jacobson A. Linking mRNA turnover and translation: assessing the polyribosomal association of mRNA decay factors and degradative intermediates. Methods 1999;17:28–37. [PubMed: 10075880]

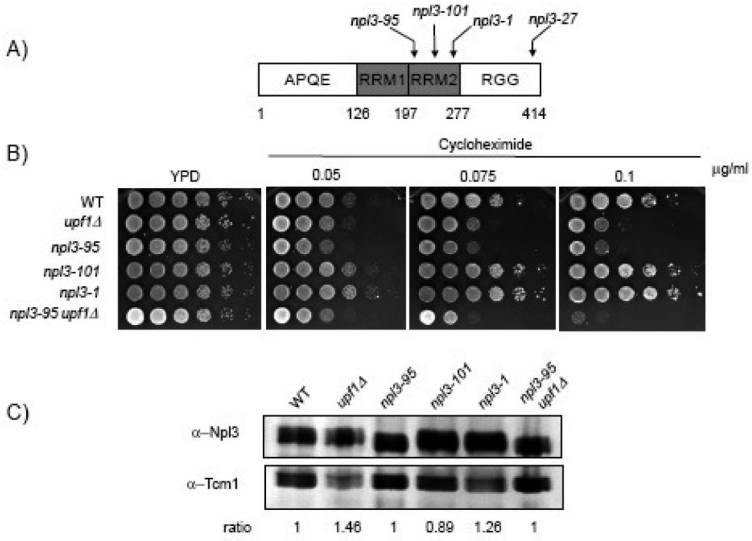

Figure 1. Npl3p plays a role in translation

(A) Schematic diagram of Npl3p showing the two RNA binding motifs (RRMs) located in the central portion of the polypeptide, the APQE motif in the N-terminal end and the RGG repeats in the carboxyl end. The arrows show the location of the three mutant alleles (*npl3-95*, *npl3-101*, *npl3-1* and *npl3-27*) in the RRM2 that were used in this study. B) Ten-fold serial dilutions of yeast cells spotted onto YPD or YPD media containing various concentrations (0.05 g/ml, 0.075 g/ml or 0.10 g/ml) of cycloheximide are shown. Plates were incubated for three days at 24°C. C) Western blot analysis was performed with lysates from WT, *upf1Δ*, *npl3-95*, *npl3-101*, *npl3-1* and *npl3-95*/*upf1Δ* yeast strains. Ten micrograms of total protein extracts were immunoblotted with antibodies against Npl3p and Tcm1p (ribosomal protein control).

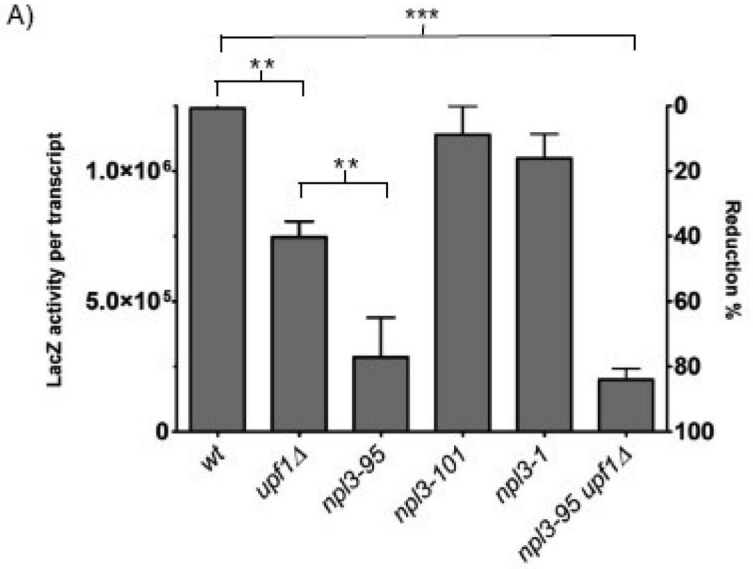

Figure 2. General translation rates of the *npl3* mutant strains

A) Wild-type control (WT), *upf1Δ*, *npl3-95*, *npl3-101* and *npl3-1* strains were transformed with a *lacZ* reporter construct and β-galactosidase assays were performed. *LacZ* activity is expressed in β-galactosidase units per transcript for each strain used in the analysis. Total *lacZ* activity was normalized to total *lacZ* mRNA levels (activity per transcript). The *LacZ/mRNA* activity obtained for the wild-type strain was set as 100% and used as a reference point for comparison. n = 3 independent experiments. Error bars represent 1 SEM above and below the mean. * $p < 0.05$, ** $p < 0.001$, *** $p < 0.0001$.

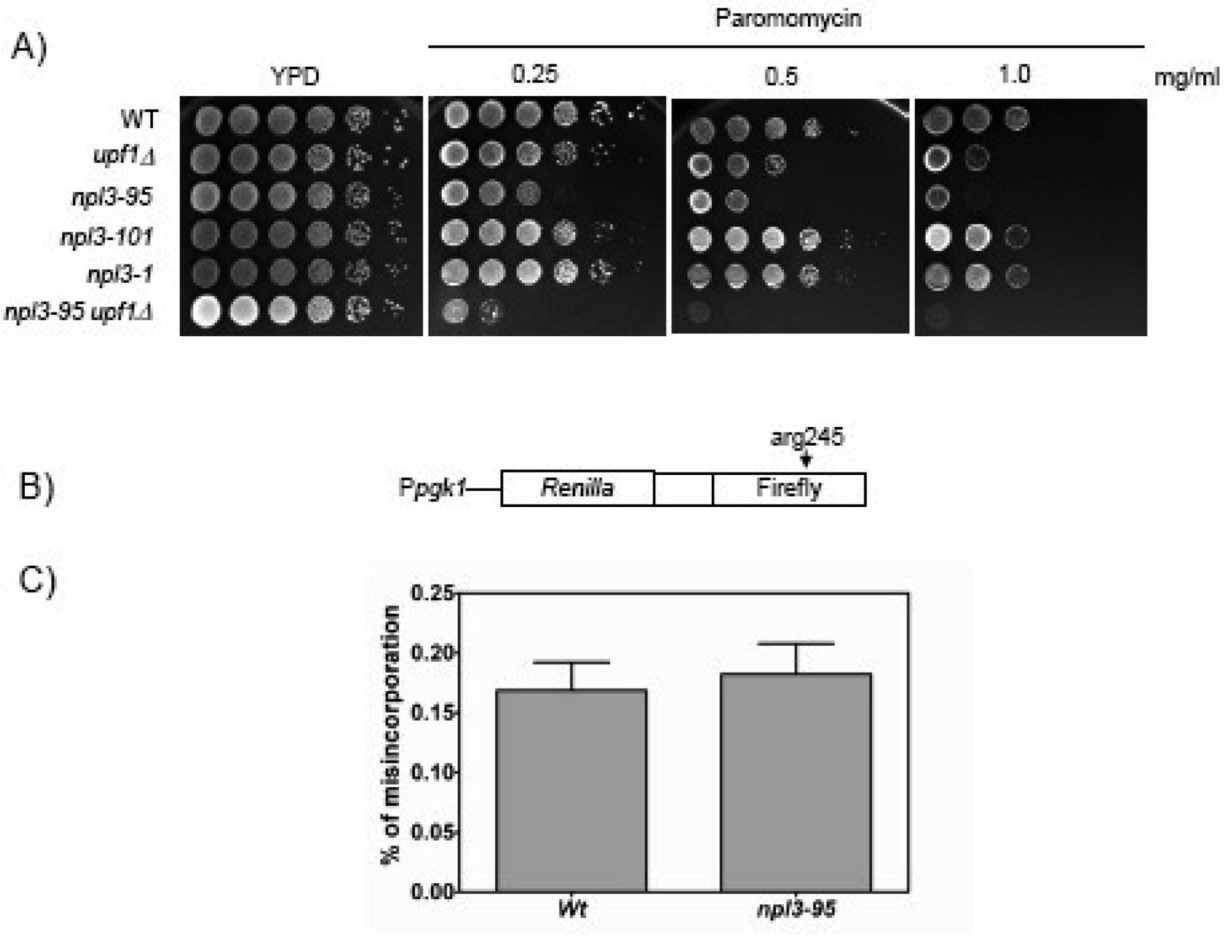

Figure 3. The *npl3-95* mutant allele is sensitive to paromomycin

A) Ten-fold serial dilutions of various yeast strains spotted on YPD or YPD media containing 0.25 mg/ml, 0.50 mg/ml or 1.0 mg/ml of the translational inhibitor paromomycin. Cells were incubated for three days at 24°C. B) Schematic diagram of the dual luciferase reporter chimera used to measure translation elongation fidelity. C) The percentage of elongation misincorporation was expressed as wild-type or mutant Firefly/*Renilla* luciferase activity. No significant difference on translation elongation fidelity was observed between the wild type *NPL3* and mutant *npl3-95* strains ($P = 0.7108$).

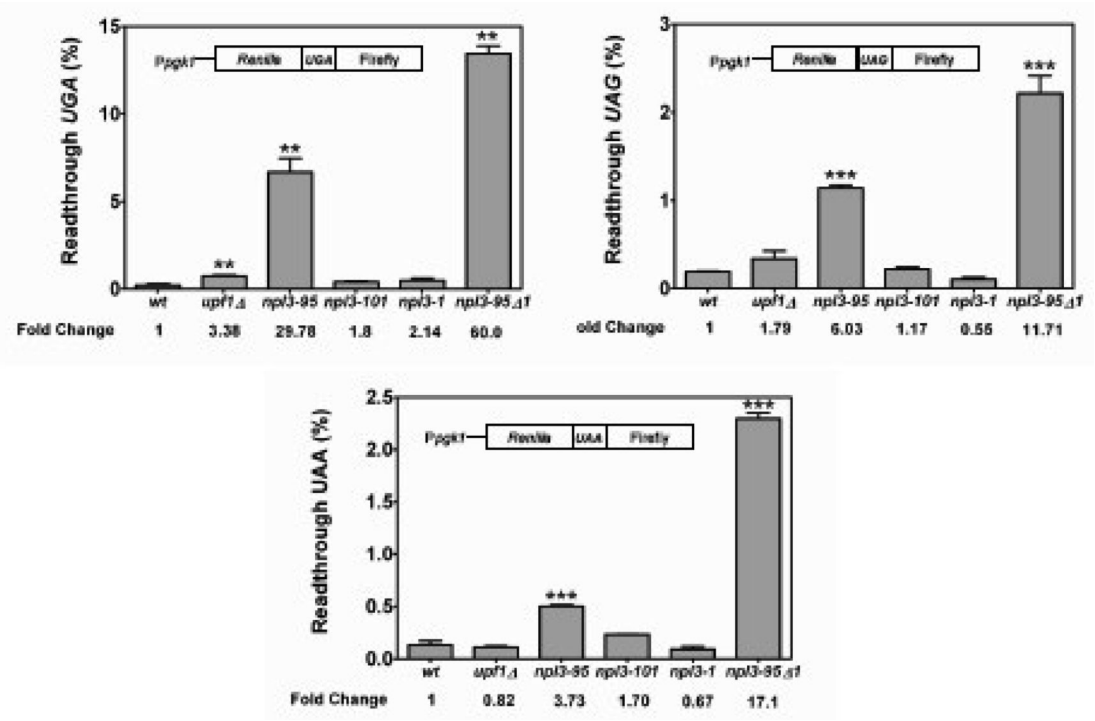

Figure 4. *npl3-95* cells display defects in translation fidelity

A) Dual luciferase assays were conducted to determine the efficiency of stop codon recognition (UAA, UAG, or UGA). The percentage of translational readthrough for each strain was calculated as the Firefly/Renilla luciferase activity (nonsense) divided by the Firefly/Renilla luciferase activity (sense) multiplied by 100. Two tailed t-tests were used for statistical testing. n = 3 for all experiments shown (the asterisk indicates a statistically significant result when compared to the wild type strain).

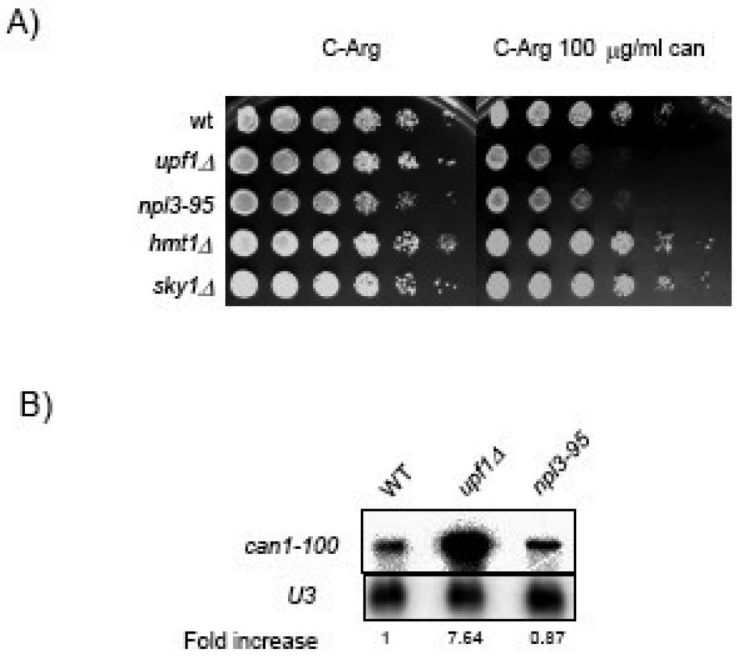

Figure 5. *hmt1Δ* or *sky1Δ* strains do not display nonsense suppression phenotypes

A) Ten-fold serial dilutions of yeast suspensions with similar cell numbers from the indicated strains were plated on C-Arg (left panel) and C-Arg containing 100 g/ml of canavanine (right panel). Cells were incubated for three days at 24°C. B) Northern blot analysis of the *can1-100* nonsense-containing mRNA measured in wild type, *upf1Δ* and *npl3-95* strains.

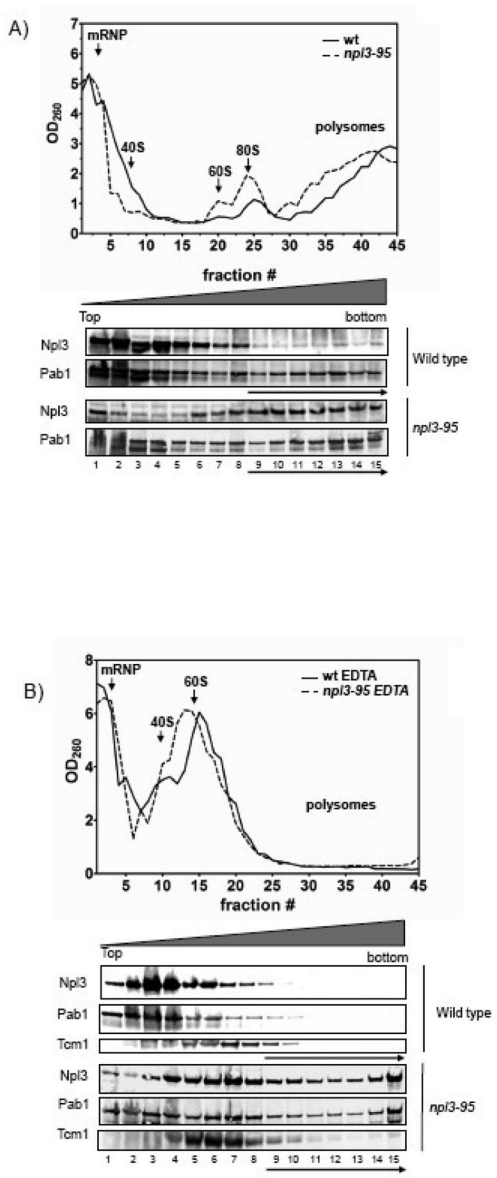

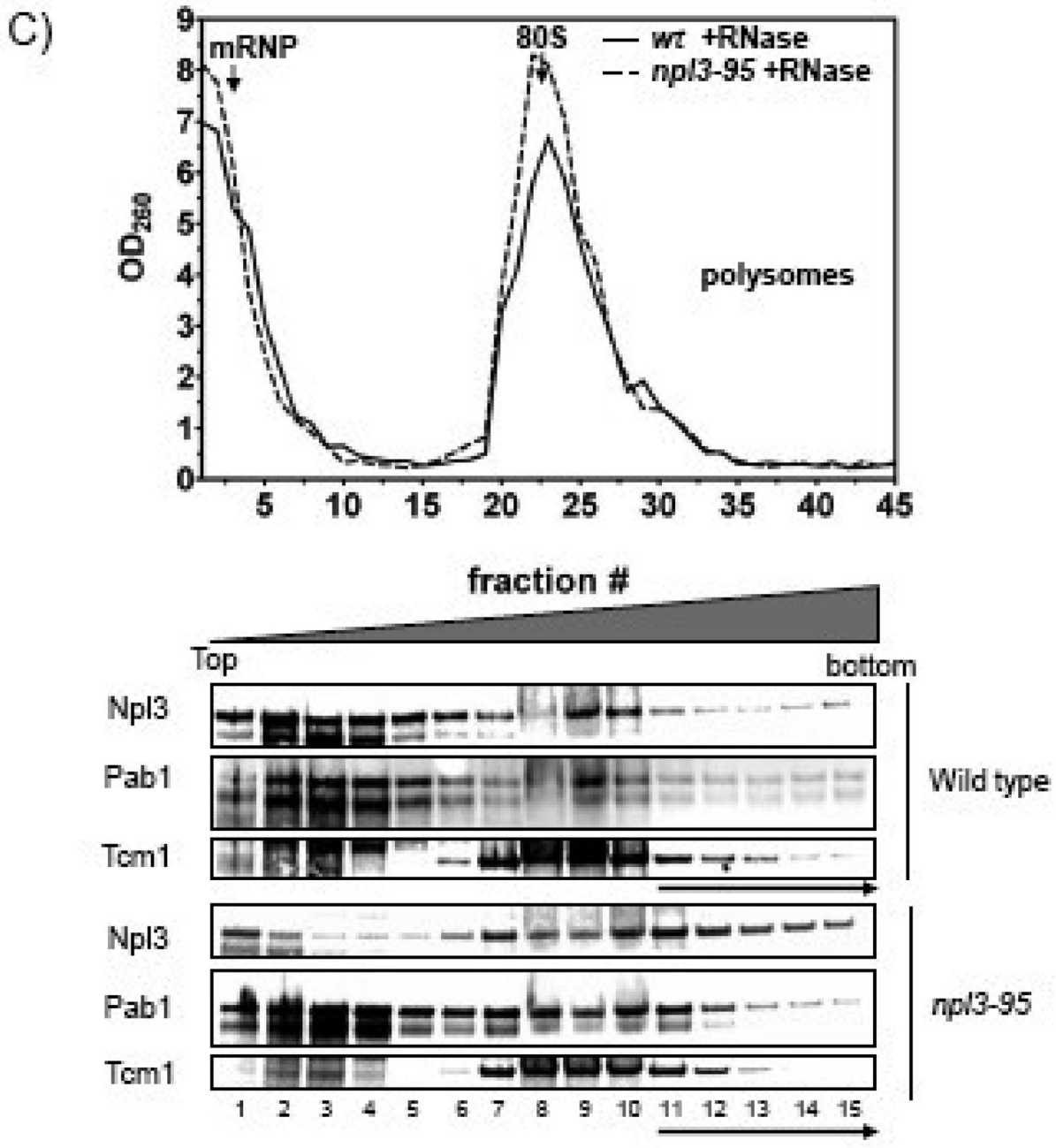

Figure 6. Cells harboring the *npl3-95* allele form heavy mRNP arrangements

The OD_{260} plot shows the UV absorption pattern from the sucrose gradient for wild type and *npl3-95*. The lower panels show Western blot analysis of the pooled fractions with antibodies against Npl3p and Pab1p. High density fractions refer to fractions 9 and above (except for the RNaseA experiment in which we the high density fractions refer to fractions 11 and above), these fractions are indicated with an arrow. Each protein lane represents three fractions from the UV plots that were pooled together. A) Distribution of Npl3p and Pab1p on sucrose density gradients. B) Polysome profile of wild type and *npl3-95* extracts treated with 15 mM EDTA. C) Polysome profile of wild type and *npl3-95* extracts treated with RNaseA (0.1 g/ml). Similar results were obtained in at least two independent experiments.

Table 1

Yeast strains used in this study.

Strains	source	Genotype
YCG9	This study	*MATa leu2-3 can1-100 ura3-1 ade2-1 his3-11,15 trp1-1*
YCG11	*Henry et. al.*	*Matα leu2-3 can1-100 ura3-1 ade2-1 his3-11,15 trp1-1 npl3-101*
YCG12	*Henry et. al.*	*MATa leu2-3 can1-100 ura3-1 ade2-1 his3-11,15 trp1-1 npl3-95*
YCG16	*Henry et. al.*	*Matα his3-11 ade2-1 leu2-1 ura3-1 npl3-1*
YCG25	*Henry et. al.*	*MATa ade2-1 his3-11, 15 leu2-3, 112 trp1-1 ura3-1 can1-100 upf1::HIS3*
YCG35	This study	*MATa ade2-1 his3-11, 15 leu2-3, 112 trp1-1 ura3-1 can1-100 upf1::his5 npl3-95*
YCG46	This study	*MATa ade2-1 his3-11, 15 leu2-3, 112 trp1-1 ura3-1 can1-100 sky1::HIS3*
YCG47	This study	*MATa ade2-1 his3-11, 15 leu2-3, 112 trp1-1 ura3-1 can1-100 hmt1::HIS3*

Table 2

Plasmids used in this study.

Plasmids	source	Plasmid description
pCG95	*Salas-Marco et.al.*	*URA3* vector CAAA control for pCG96.
pCG96	*Salas-Marco et.al*	*URA3* vector UAAA stop codon.
pCG97	*Salas-Marco et.al*	*URA3* vector CAGC control for pCG98.
pCG98	*Salas-Marco et.al*	*URA3* vector UAGC stop codon.
pCG99	*Salas-Marco et.al*	*URA3* vector CGAC control for pCG100.
pCG100	*Salas-Marco et.al*	*URA3* vector UGAC stop codon.
pCG106	*Pappas et. al.*	*PGK1* (*TATA*)-*lacZ URA3*.
pCG107	*Salas-Marco et.al*	Dual luciferase assay reporter for missincorporation. Firefly luciferase H245 (CAC to CGC).